

Anti-proliferative and Antioxidant Activities of 1-methoxy-3-methyl-8-hydroxy-anthraquinone, a Hydroxyanthraquinoid Extrolite Produced by *Amycolatopsis thermoflava* strain SFMA-103

C. Ganesh Kumar^{1*}, Poornima Mongolla^{1,4}, Cheemalamarri Chandrasekhar^{1,4}, Yedla Poornachandra¹, Bandi Siva², K. Suresh Babu², and Kallaganti Venkata Siva Ramakrishna³

¹Medicinal Chemistry and Biotechnology Division, ²Natural Products Chemistry Division, ³Nuclear Magnetic Resonance Centre, CSIR-Indian Institute of Chemical Technology, Uppal Road, Hyderabad 500007, India

⁴Department of Biotechnology, Acharya Nagarjuna University, Nagarjunanagar, Guntur 522510, India

Received: May 4, 2017 / Accepted: June 26, 2017

Actinobacteria are prolific producers of a large number of natural products with diverse biological activities. In the present study, an actinobacterium isolated from sunflower rhizosphere soil sample collected from Medak, Andhra Pradesh, South India was identified as *Amycolatopsis thermoflava* strain SFMA-103. A pigmented secondary metabolite in culture broth was extracted by using methanol and it was further purified by silica gel column chromatography with methanol-chloroform solvent system. Structural elucidation studies based on UV-visible, 1D and 2D-NMR, FT-IR, and mass spectroscopic analyses confirmed the structure as 1-methoxy-3-methyl-8-hydroxy-anthraquinone. It showed significant in vitro anticancer activity against lung cancer and lymphoblastic leukemia cells with IC₅₀ values of 10.3 and 16.98 μM, respectively. In addition, 1-methoxy-3-methyl-8-hydroxy-anthraquinone showed good free radical scavenging activity by DPPH method with an EC₅₀ of 18.2 μg/ml. It also showed other promising superoxide radical scavenging, nitric oxide radical scavenging and inhibition of lipid peroxidation activities. This is a first report of anti-proliferative and antioxidant activities of 1-methoxy-3-methyl-8-hydroxy-anthraquinone isolated from *A. thermoflava* strain SFMA-103 which may find potential application in biotechnological and pharmaceutical fields.

Keywords: Anthraquinone, *Amycolatopsis thermoflava*, extrolite, antitumor, antioxidant

Introduction

Soil comprises of a myriad of ecosystems harbouring diverse microorganisms, including bacteria, actinobacteria, fungi, etc. The continuous search for novel microbes from different soils around the world has resulted in the discovery of numerous bioactive compounds exhibiting a

diverse array of biological activities for the treatment of various diseases. Bioprospecting is a term recently coined to refer to the search for novel products or microorganisms of economic importance from the world's biota. The class actinobacteria accounts for a significant proportion of soil microflora and are widely distributed in both natural and man-made environments. Actinobacteria are considered as a rich repertoire of diverse bioactive secondary metabolites (extrolites) and have gained increased attention since many of the clinically important antibiotics are produced by some rare genera

*Corresponding author

Tel: +91-40-27193105; Fax: +91-40-27193189

E-mail: cgkumar@iict.res.in

© 2017, The Korean Society for Microbiology and Biotechnology

of actinobacteria, including vancomycin by *Amycolatopsis orientalis*, rifamycin B from *Amycolatopsis mediterranei*, gentamicin C produced by *Micromonospora purpurea*, erythromycin A by *Saccharopolyspora erythraea* and teicoplanin by *Actinoplanes teichomyceticus* [1]. Out of >8000 bioactive products recorded in the ABL database, 45.6% bioactives are produced by the prolific bioactive producers catering to the genus *Streptomyces* alone and 16% bioactives are produced by strains belonging to the rare genera of actinobacteria [2]. As the search for novel bioactive compounds continues, it has become apparent that the rate of discovery of new compounds from terrestrial streptomycetes has decreased to a large extent, whereas the rate of re-isolation of known compounds has increased [3]. Considering this fact, the emphatic search in the recent years has been reoriented towards actinobacteria from normal habitats and/or to discover new strains/species from diverse niches. The rationale behind such a strategy is to increase the probability of identifying novel chemical entities by screening actinobacteria which were less focused in the previous natural product screening programs, since the isolation frequency of rare actinobacteria is much lower than that of the streptomycete strains isolated by conventional methods [2].

Bioactive extrolites such as anthraquinoid derivatives have a basic structure of 9,10-anthracenedione, i.e., a tricyclic aromatic compound with ketone groups present on the central ring in position C-9 and C-10. The functional groups, particularly hydroxyl, attached at specific positions have resulted in many anthraquinoid derivatives with diverse pharmacological applications [4]. Reports on anthraquinone-based extrolites from actinobacteria are very limited which include actinorhodin, a benzoisochromanone polyketide antibiotic produced by *Streptomyces coelicolor* A3(2) [5]; blanchaquinone from *Streptomyces* strain MST-77755 [6]; tetracenomycin D from *Streptomyces corchorusii* AUBN(1)/7 [7]; lupinacidins A and B from endophytic *Micromonospora* sp. [8]; four anthraquinone derivatives such as 2-ethyl-1,8-dihydroxy-3-methyl-anthraquinone, 2-ethyl-1-hydroxy-8-methoxy-3-methyl anthraquinone, 3,8-dihydroxy-1-propylantraquinone and propylantraquinone-2-carboxylic ester from *Micromonospora rhodorangea* [9]; 2,3-dihydroxy-9,10-anthraquinone from *Streptomyces galbus* ERINLG-127 [10] and 2-hydroxy-9,10-anthraqui-

none from *Streptomyces olivochromogenes* ERINLG-261 [11]. In the present study, purification, structural elucidation and evaluation of cytotoxic and antioxidant activities of 1-methoxy-3-methyl-8-hydroxy-anthraquinone from *Amycolatopsis thermoflava* strain SFMA-103 were carried out.

Materials and Methods

Microorganism and growth conditions

The actinobacterium strain SFMA-103 was previously isolated in our laboratory from the rhizosphere soil sample from sunflower (*Helianthus annuus* L.) fields collected from Medak, Telangana, South India employing soil dilution technique on glycerol-asparagine-salts agar medium. The strain was maintained on yeast extract-malt extract-dextrose (YMD) agar medium at 4°C for further study.

Morphological, cultural and molecular characterization

Cultural and morphological characteristics of the strain was studied according to standard procedures on International Streptomyces Project (ISP) media such as tryptone-yeast extract agar (ISP-1), YMD agar (ISP-2), oat meal agar (ISP-3), starch-inorganic salts agar (ISP-4), glycerol-asparagine-salts agar (ISP-5), peptone-yeast extract iron agar (ISP-6), tyrosine agar (ISP-7) and non-ISP media like nutrient agar and Czapek-Dox agar media and incubated at 35°C for 7 days [12]. The micro-morphology of the strain cultured on ISP medium 2 at 40°C for 5 days was examined under a light microscope [13]. Morphological properties such as colony characteristics, type of aerial hyphae, and growth of vegetative hyphae, fragmentation and colour pattern and spore formation were observed [14].

Extraction of genomic DNA of the strain was performed according to the method described by Rainey and coworkers [15]. The 16S rRNA gene was amplified using forward primer (5'-AGA GTT TGA TCM TGG CTC AG-3') and the reverse primer (5'-AAG GAG GTG WTC CAR CC-3') on a PCR using an initial denaturation step at 98°C for 3 min, followed by 35 cycles of denaturation at 94°C for 1 min, primer annealing at 54°C for 1 min, and primer extension at 72°C for 2 min. The final cycle was achieved by a 5 min extension step at 72°C and the PCR product was analyzed in 1% agarose gel. The amplified

1.5 kb PCR product was eluted from the agarose gel using the GenElute™ gel extraction kit (Sigma-Aldrich, USA) and was sequenced on a ABI 3730XL DNA analyzer (Applied BioSystems, USA). The phylogenetic position of the isolate (SFMA-103) was determined by performing a nucleotide sequence database search using the BLASTN program of NCBI database. The evolutionary history was inferred by using the Maximum Likelihood method based on the Tamura-Nei model [16]. The tree with the highest log likelihood (-5843.1440) is shown. The percentage of trees in which the associated taxa clustered together is shown next to the branches. Initial tree(s) for the heuristic search were obtained automatically by applying Neighbor-Joining and BioNJ algorithms to a matrix of pairwise distances estimated using the Maximum Composite Likelihood (MCL) approach, and then selecting the topology with superior log likelihood value. The tree is drawn to scale, with branch lengths measured in the number of substitutions per site. The analysis involved 32 nucleotide sequences. Codon positions included were 1st + 2nd + 3rd + non-coding. All positions with less than 95% site coverage were eliminated. That is, fewer than 5% alignment gaps, missing data, and ambiguous bases were allowed at any position. There were a total of 1370 positions in the final dataset. Evolutionary analyses were conducted using MEGA6 software [17].

Fermentation, isolation and purification of the extrolite

Strain SFMA-103 was cultured in glycerol-asparagine-salts medium (pH 7.0) and incubated at 40°C with agitation at 150 rpm in a New Brunswick Innova 43R shaker (Eppendorf North America, Hauppauge, USA) for 5 days. The fermented medium was later subjected to centrifugation (Sorvall RC 5C Plus, Kendro Lab Products, USA) at 8200 ×g to remove the cell biomass resulting in the cell-free supernatant. The extrolites present in the cell-free supernatant were extracted by absorption onto Diaion HP-20 (3%) resin. The resin was washed with water and then extracted with methanol to obtain the crude extract fractions. The fractions were analyzed by thin-layer chromatography (TLC) on silica gel 60 plates (F₂₅₄). Plates were developed in a methanol-chloroform (10:90, v/v) solvent mixture and visualized under UV light at 254 nm which revealed the presence of a single spot. Further, the crude extract fractions containing

the extrolite were pooled, concentrated under reduced pressure on a rotary vacuum evaporator (Rotavapor R-205, Büchi, Switzerland) and further profiled by silica gel (60–120 mesh) column (3 × 60 cm) chromatography. The extrolite was eluted with a linear gradient of methanol-chloroform solvent system (0.5:95, v/v). The same solvent mixture was continued till the extrolite was completely eluted and after drying resulted in golden yellow wax.

Structural characterization of the extrolite

The UV spectrum was measured by dissolving the purified extrolite in spectroscopic acetonitrile and recorded at 30°C on a UV-visible double-beam spectrophotometer (Lambda 25, Perkin-Elmer, USA). 1D and 2D-NMR spectra were recorded on a Bruker Avance 300 and 600 MHz NMR spectrometers (Bruker, Switzerland) in DMSO-d₆ at room temperature, and chemical shifts were represented in δ values expressed in ppm with tetramethylsilane as the internal standard. The Fourier transform infrared (FT-IR) spectrum was recorded using the Thermo-Nicolet Nexus 670 FT-IR spectrophotometer (ThermoFisher Scientific Inc., USA) at a resolution of 4 cm⁻¹ in the wavenumber region of 400–4,000 cm⁻¹. ESI-MS spectrum was recorded on a QSTAR XL Hybrid ESI-Q TOF mass spectrometer (Applied Biosystems Inc., USA).

Antioxidant assays

Antioxidant activity of purified extrolite was assessed on the basis of the free radical scavenging effect of the stable 1, 1-diphenyl-2-picrylhydrazyl (DPPH) with some modifications of a previously described method [18]. The diluted working solution of the purified extrolite was prepared in methanol. One millilitre of DPPH (0.002% prepared in methanol) was mixed with 1 ml of purified extrolite at different concentrations ranging from 10, 20, 40, 60, 80 and 100 µg/ml. The mixtures were shaken vigorously and left to stand in dark for 30 min. Absorbance of the reaction mixtures were measured at 517 nm on a UV-visible spectrophotometer (Lambda 25, Perkin-Elmer, USA). Butyl hydroxytoluene (BHT) and α-tocopherol were run in parallel as positive controls. The radical scavenging activity was measured as a decrease in the absorbance of DPPH. Lower absorbance of the reaction mixture indicated higher free radical scavenging activity. DPPH radical scavenging activity was cal-

culated using the formula [19]: DPPH radical scavenging activity (%) = [(Absorbance of control – Absorbance of test sample) / (Absorbance of control)] × 100. The absorbance of DPPH was plotted against the antioxidant concentrations as standard curve to calculate the radical scavenging activity. Radical scavenging potential was expressed as EC₅₀ value, which represents the concentration of purified extrolite at which 50% of the DPPH radicals scavenged. All tests were performed in triplicate and the values are represented as mean ± SD.

The superoxide radical scavenging activity of purified extrolite was performed according to the protocol described by Liu and coworkers [20]. The superoxide radicals were generated by phenazine methosulfate - nicotinamide adenine dinucleotide (PMS/NADH) system, which reduced nitroblue tetrazolium (NBT) to form a purple coloured formazan. Butyl hydroxytoluene (BHT) and α-tocopherol were run in parallel as positive controls. The scavenging activity of superoxide radical (%) was calculated from the plotted absorbance data for the dose-response curves and the IC₅₀ values (in μM) were expressed as the mean of three independent experiments and the values are represented as mean ± SD.

The inhibition of lipid peroxidation was assayed by measuring the lipid peroxide decomposition product malondialdehyde (MDA), based on reaction with thiobarbituric acid using egg yolk as oxydizable substrate [21]. Butyl hydroxytoluene (BHT) and α-tocopherol were run in parallel as positive controls. The inhibition of lipid peroxidation was calculated from the plotted absorbance data for the dose-response curves and the IC₅₀ values (in μM) were expressed as the mean of three independent experiments and the values are represented as mean ± SD. The nitric oxide (NO) scavenging assay was performed using the modified method of Marcocci *et al.* [22], which is based on release of nitric oxide from sodium nitroprusside and quantified by the Griess reaction. Varying concentrations of pure extrolite were solubilized in methanol and to these solutions, sodium nitroprusside (400 μl) and Griess reagent (220 μl) were added, followed by incubation at 25°C for 1 h and then distilled water (2 ml) was added to each of these reaction mixtures. The absorbance was recorded at 546 nm and the IC₅₀ values were calculated from dose-response curve. All tests were performed as three independent experiments and the results were expressed as

mean ± SD.

MTT cytotoxicity assay

The cytotoxicity of pure extrolite was studied using the 3-[4,5-dimethylthiazol-2-yl]-2,5-diphenyltetrazolium bromide (MTT) viability assay [23] which was determined on the basis of measurement of in vitro growth inhibition of tumor cell lines in 96 well plates by cell-mediated reduction of tetrazolium salt to water insoluble formazan crystals using doxorubicin as a standard. The cytotoxicity was assessed against a panel of different human tumor cell lines: A549 derived from human alveolar adenocarcinoma epithelial cells (ATCC No. CCL-185), MDA-MB-231 derived from human breast adenocarcinoma cells (ATCC No. HTB-26), DU145 derived from human prostate carcinoma (ATCC No. HTB-81), HepG2 derived from human hepatocellular carcinoma (ATCC No. HB-8065), COLO 205 derived from human colon carcinoma (ATCC No. CCL-222), MOLT-4 derived from human lymphoblastic leukemia cells (ATCC No. CRL-1552) and HEK293 derived from human normal embryonic kidney cells (ATCC No. CRL-1573). Briefly, 1 × 10⁶ cells/well were seeded in 100 μl of DMEM and/or RPMI supplemented with 10% FBS in each well of 96-well microtitre plates and incubated for 24 h at 37°C in a humidified 5% CO₂ incubator (Model 2406, Shellab CO₂ incubator, USA). The purified extrolite, diluted to the desired concentrations in culture medium, was added to the wells with respective vehicle control. After 48 h of incubation, the cells were subjected to MTT assay (5 mg/ml MTT) and the plates were further incubated for 2 h. The supernatant from each well was carefully removed, formazan crystals were dissolved in 100 μl of DMSO and absorbance was recorded at a wavelength of 540 nm on a multimode microplate reader (Infinite[®] M200, Tecan, Switzerland). The IC₅₀ values (50% inhibitory concentration) were calculated from the plotted absorbance data for the dose-response curves. IC₅₀ values (in μM) were expressed as the average of three independent experiments and the results were expressed as mean ± SD.

Results and Discussion

Taxonomy of strain SFMA-103

Morphological and cultural characteristics of strain SFMA-103 are recorded in Table 1. The strain exhibited

luxuriant growth on ISP-5 and good growth on ISP-1, ISP-2, ISP-4 and nutrient agar. The growth was moderate on ISP-3 and ISP-7, while poor growth was observed on ISP-6 and Czapek Dox medium. A prominent golden yellow pigment production was observed on ISP-5 medium. Micromorphology of the strain grown on ISP medium 2 showed light grey aerial mycelium with light yellow colored substrate mycelium that fragmented into rod-shaped elements, which is the characteristic feature of *Amycolatopsis* sp. [13]. The phylogenetic position of the strain was determined by amplifying the 16S rRNA region and sequence of the strain was examined by BLAST analysis. The results revealed that the strain belongs to the genus *Amycolatopsis*, the suborder *Pseudonocardineae* of the family *Pseudonocardiaceae*. Based on the phylogenetic tree (Fig. 1), the 16S rRNA genome sequence of the strain showed similarity with different *Amycolatopsis* strains. Based on the sequence homology, the strain SFMA-103 showed identity with both *Amycolatopsis eurytherma* strain NT202 [24] and *A. thermoflava* N1165 [13]. However, it is reported that *A. eurytherma* strain NT202 showed no pigment production, while *A. thermoflava* N1165 showed soluble yellow pigment production which corroborates with the observations made in the present study. Based on these comparisons, the strain SFMA-103 was identified as *A. thermoflava* and the 16S rRNA sequence is submitted with Genbank accession number JN378749. The strain SFMA-103 is maintained in the in-house culture collection of the laboratory and designated as *A. thermoflava* strain ICTA-103.

Isolation, purification and identification of the bioactive extrolite

The fermentation of strain SFMA-103 was carried out in glycerol-asparagine-salts medium which produced the extrolite after 5 days of incubation. The culture filtrate revealed the presence of a single major spot on the TLC plate developed in a solvent mixture of methanol-chloroform (10:90, v/v). The extrolite was extracted in methanol to obtain a crude extract (1.2 g/l) and purified by silica gel column chromatography in a solvent system of methanol-chloroform (0.5:95, v/v). The extrolite on the TLC plate was UV-active when visualized under UV light at a wavelength of 254 nm and was developed by spraying with anisaldehyde reagent followed by heating at 100°C for 2–3 min which appeared as a blue coloured spot.

The pure extrolite was obtained as orange yellow coloured wax (30 mg/l) and the molecular formula of $C_{16}H_{12}O_4$ was deduced based on EI-MS data, which showed a molecular ion peak at m/z 268.99 $[M + H]^+$ [calcd. For $C_{16}H_{12}O_4$, 269, $M + H]^+$. UV (MeOH) scan spectrum of the purified extrolite showed absorbance peaks at 206, 287 and 420 nm. FT-IR spectrum of the purified extrolite showed a strong hydroxyl group absorption band at 3400 cm^{-1} , together with one carbonyl group absorption band at 1558 cm^{-1} , suggesting the presence of hydroxyl and quinone groups. ^1H NMR (300 MHz, DMSO- d_6) showed an ABX coupling system for aromatic signals at δ (ppm) 11.48 (1H, s, OH-1), 7.74 (1H, t, $J = 8.4$ and 6.7 , H-6), 7.49 (1H, d, $J = 8.4$, H-7), 7.36 (1H, s, H-4), 7.32 (1H, d, $J = 6.7$, H-5), 7.13 (1H, s,

Table 1. Cultural characteristics of strain SFMA-103 on different International Streptomyces Project (ISP) and non-ISP media.

Culture medium	Growth pattern	Reverse colony colour	Aerial mycelium colour and growth	Pigment production
ISP-1	Good	Light yellow	White sporulation	No pigment production
ISP-2	Good (penetration into the medium)	Light yellow	Light gray	No pigment production
ISP-3	Moderate growth	Light yellow	Light grayish sporulation	No pigment production
ISP-4	Good	Light yellow	White sporulation	Yellow
ISP-5	Luxuriant growth	Dark brown	Off white sporulation	Golden yellow pigment
ISP-6	Poor growth	Colour less	Colour less	No pigment production
ISP-7	Moderate growth	Pale yellow	White sporulation	No pigment production
Nutrient agar	Good	Light yellow	White sporulation	Yellow
Czapek Dox	Poor growth	Colour less	Colour less	No pigment production

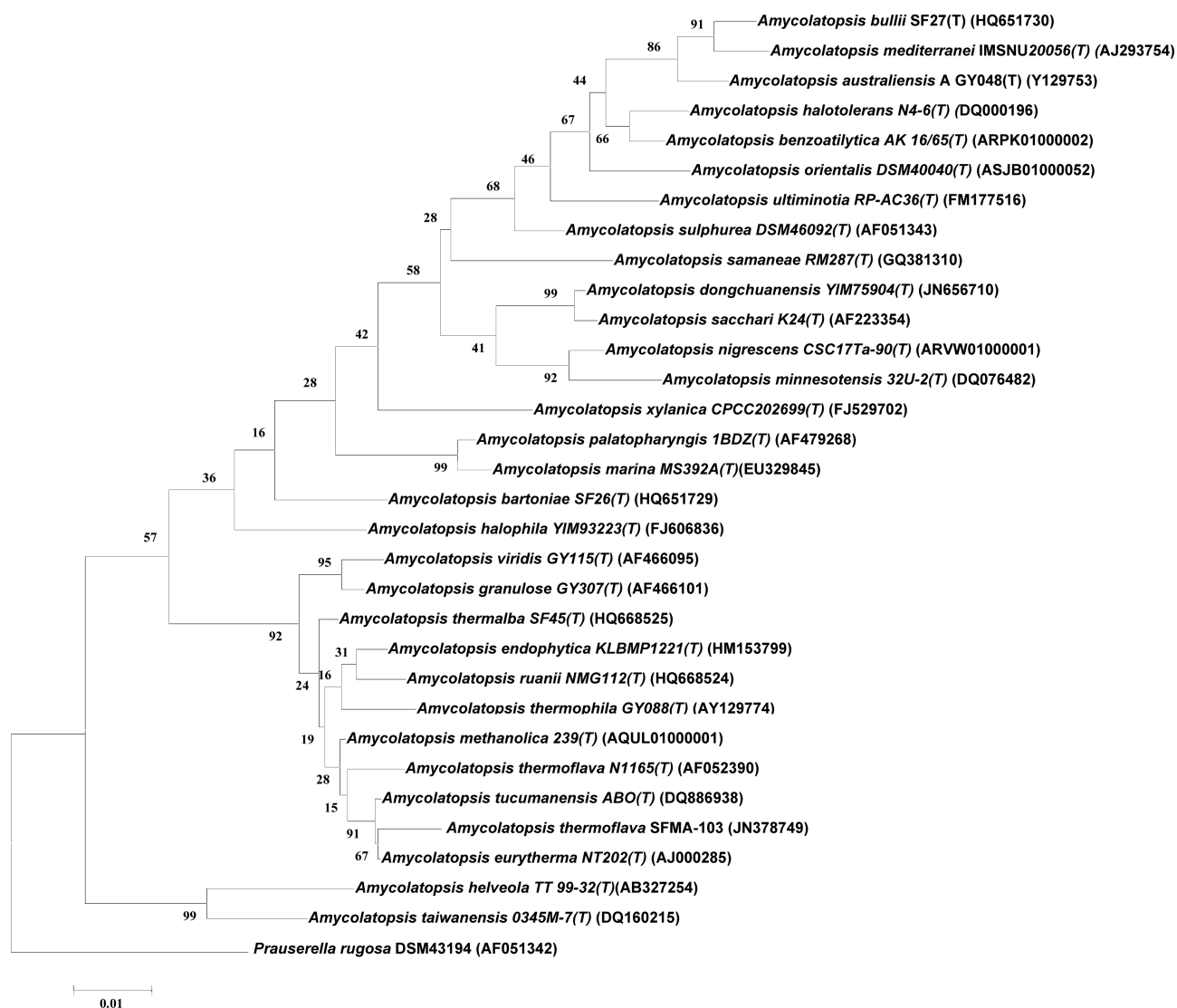


Fig. 1. Molecular phylogenetic analysis by maximum-likelihood method.

H-2), 2.40 (3H, s, H₃-3) and 3.69 (3H, s, OMe). The ¹³C NMR (75 MHz, DMSO-d₆) showed the presence of two ketals carbons with chemical shifts, δ (ppm): 184.9 (C-9) and 182.4 (C-10), twelve aromatic carbons with chemical shifts, δ (ppm): 160.89 (C-8), 156.9 (C-1), 139.0 (C-13), 137.2 (C-6), 132.5 (C-11), 128.0 (C-14), 123.0 (C-7), 122.34 (C-4), 118.8 (C-3), 118.5 (C-5), 115.5 (C-2), 113.7 (C-12), methoxy group at δ 55.9 ppm and one aromatic methyl group at δ 21.1 ppm, which is characteristic of an anthraquinone chromophore. The key HMBC and COSY correlations for the pure extrolite is shown in Fig. 2. Based on the 1D and 2D NMR, FT-IR and mass spectral

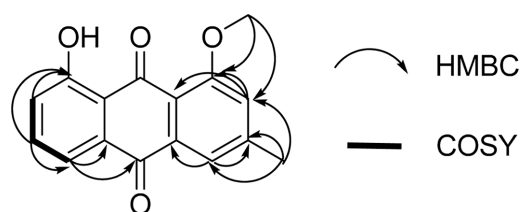


Fig. 2. Key HMBC and COSY correlations of 1-methoxy-3-methyl-8-hydroxy-anthraquinone.

data (Figs. S1–S10), the chemical structure (Fig. 3) of the pure extrolite was determined as 1-methoxy-3-methyl-8-hydroxy-anthraquinone. Literature search

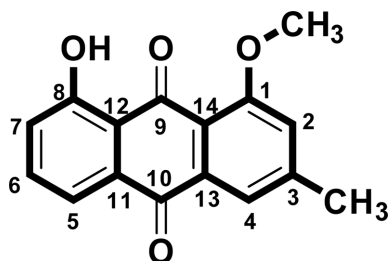


Fig. 3. Chemical structure of 1-methoxy-3-methyl-8-hydroxy-anthraquinone.

revealed that there are no reports on this anthraquinone from any microbial source.

Effect of 1-methoxy-3-methyl-8-hydroxy-anthraquinone on antioxidant activity

Considering the pharmacological importance of plant-derived anthraquinones [25], the pure extrolite from *A. thermoflava* was assayed for antioxidant and anti-tumor activities. 1-methoxy-3-methyl-8-hydroxy-anthraquinone scavenged DPPH free radicals, superoxide anions, nitric oxide radicals and lipid peroxy radicals in a dose-dependent manner as compared to the positive controls, BHT and α -tocopherol (Table 2). DPPH is an oxidizing radical

Table 2. Antioxidant activities of 1-methoxy-3-methyl-8-hydroxy-anthraquinone produced by *A. thermoflava* SFMA-103.

Test compound	EC ₅₀ (μ g/ml) (Mean \pm SD)
DPPH radical scavenging activity	
1-methoxy-3-methyl-8-hydroxy-anthraquinone	18.2 \pm 0.41
Butyl hydroxytoluene (Positive control)	28.7 \pm 0.24
α -Tocopherol (Positive control)	10.6 \pm 0.32
Superoxide free radical scavenging activity	
1-methoxy-3-methyl-8-hydroxy-anthraquinone	11.9 \pm 0.39
Butyl hydroxytoluene (Positive control)	13.1 \pm 0.22
α -Tocopherol (Positive control)	6.8 \pm 0.39
Nitric oxide (NO) radical scavenging activity	
1-methoxy-3-methyl-8-hydroxy-anthraquinone	72.8 \pm 0.25
Butyl hydroxytoluene (Positive control)	74.2 \pm 0.11
α -Tocopherol (Positive control)	52.8 \pm 0.19
Inhibition of lipid peroxidation	
1-methoxy-3-methyl-8-hydroxy-anthraquinone	31.4 \pm 0.18
Butyl hydroxytoluene (Positive control)	43.2 \pm 0.43
α -Tocopherol (Positive control)	21.3 \pm 0.28

that forms a stable free radical which is reduced and stabilized by antioxidants. 1-methoxy-3-methyl-8-hydroxy-anthraquinone exhibited a significant DPPH radical scavenging activity (EC₅₀ value of 18.2 \pm 0.41 μ g/ml) as compared to that of BHT, whereas α -tocopherol (positive control) exhibited a higher DPPH radical scavenging activity (EC₅₀ value of 10.6 \pm 0.32 μ g/ml). In this context, 1-methoxy-3-methyl-8-hydroxy-anthraquinone reduced the free radicals to the corresponding hydrazine when it reacted with the released hydrogen ions. Further, the 1-methoxy-3-methyl-8-hydroxy-anthraquinone showed promising superoxide free radical scavenging activity (IC₅₀ value of 11.9 \pm 0.39 μ g/ml) comparable to that of BHT and α -tocopherol (positive controls). Superoxide anions exert deleterious effects on biological system by forming singlet oxygen and hydroxyl radicals upon decomposition. The nitric oxide (NO) radical scavenging activity exhibited by 1-methoxy-3-methyl-8-hydroxy-anthraquinone was significant (IC₅₀ value of 72.8 \pm 0.25 μ g/ml) as compared to the positive controls. 1-methoxy-3-methyl-8-hydroxy-anthraquinone stabilized the lipid peroxidation product, malondialdehyde (MDA) and exerted significant inhibitory effect on lipid peroxidation with EC₅₀ value of 31.4 \pm 0.18 μ g/ml as compared to that of BHT and α -tocopherol (positive controls). In biological systems, MDA acts as a mutagen and exerts its deleterious effects by reacting with DNA bases to form DNA-DNA interstrand crosslinks or DNA-protein crosslinks [26, 27]. These results suggest that the antioxidant mechanism for 1-methoxy-3-methyl-8-hydroxy-anthraquinone possibly depends on scavenging DPPH free radicals, superoxide anions, nitric oxide radicals and lipid peroxy radicals.

Effect of 1-methoxy-3-methyl-8-hydroxy-anthraquinone on cytotoxicity

The *in vitro* cytotoxicity of 1-methoxy-3-methyl-8-hydroxy-anthraquinone was evaluated on a panel of seven tumour cell lines, i.e. A549 (lung cancer), MDA-MB-231 (Breast cancer), DU145 (prostate cancer), HepG2 (liver cancer), COLO 205 (colon cancer), MOLT-4 (lymphoblastic leukemia) and HEK293 (normal human embryonic kidney cells) using MTT assay. Doxorubicin was used as the reference drug. The results to this regard are summarized in Table 3 and expressed as IC₅₀ values (μ M). The *in vitro* screening results revealed that

Table 3. In vitro cytotoxicity of 1-methoxy-3-methyl-8-hydroxy-anthraquinone produced by *A. thermoflava* SFMA-103.

Compound	IC ₅₀ values in (μM)						
	A549	MDA-MB-231	DU145	HepG2	COLO205	MOLT-4	HEK293 (Normal)
1-methoxy-3-methyl-8-hydroxy-anthraquinone	10.3 ± 0.2	42.3 ± 0.1	28.2 ± 0.3	- ^a	17.9 ± 0.3	17.0 ± 0.1	-
Doxorubicin	0.7 ± 0.4	0.6 ± 0.2	0.6 ± 0.2	0.6 ± 0.4	0.5 ± 0.3	0.9 ± 0.3	-

^aNo activity.

A549 - Human alveolar adenocarcinoma epithelial cells.

MDA-MB-231 - Human breast adenocarcinoma cells.

DU145 - Human prostate carcinoma.

HepG2 - Human hepatocellular carcinoma.

COLO205 - Human colon carcinoma.

MOLT-4 - Human lymphoblastic leukemia cells.

HEK293 - Normal human embryonic kidney cells.

the pure extrolite from strain SMFA-103 exhibited promising anticancer activity with IC₅₀ values ranging between 10.3–42.3 μM. Among all tested cell lines, 1-methoxy-3-methyl-8-hydroxy-anthraquinone showed significant anticancer activity against lung cancer and lymphoblastic leukemia cell lines with IC₅₀ values of 10.3 and 16.98 μM, respectively. It did not show any inhibition against the normal human embryonic kidney cell line.

Studies on some anthraquinone derivatives derived from various *Streptomyces* sp. confirm the anticancer activity towards different tumor cell lines exhibited by these natural products. Some anthraquinone extrolites like tetracenomycin D from *Streptomyces corchorusii* AUBN(1)/7 [7], galvaquinones A-C from *Streptomyces spinoverrucosus* strain SNB-032 [28] and rubimycinone A from *Streptomyces* sp. Lv-6-8 [29] exhibited varying levels of antitumor activities. 2,3-dihydroxy-9,10-anthraquinone secreted by *Streptomyces galbus* ERINLG-127 showed cytotoxicity against lung adenocarcinoma cancer cell line, A549 with IC₅₀ value of 60 μg/ml [10]. Further, 1,8-dihydroxy-2-ethyl-3-methylanthraquinone produced by *Streptomyces* sp. FX-58 showed cytotoxicity against human tumor cell lines of pro-myelocytic leukemia HL-60, gastric carcinoma BGC-823 and adenocarcinoma MDA-MB-435 with IC₅₀ values of 6.83, 82.2 and 56.59 μg/ml, respectively [30]. Antitumor anthraquinones such as lupinacidins A and B isolated from an endophytic *Micromonospora* sp. exhibited dose-dependent inhibition of in vitro invasion of colon 26-L5 cells with IC₅₀ values of 0.07 μg/ml (= 0.21 μM) and 0.3 μg/ml (= 0.92 μM), respectively. Lupinacidin A exhibited more potency both in cytotoxic and anti-invasive activities as compared to

Lupinacidin B, and the alkyl substituent contributed to these activities [8]. Saliniquinones A-F, were cytotoxic anthraquinone-γ-pyrone derivatives produced by the marine actinobacterium *Salinispora arenicola* strain CNS-325. Among them, Saliniquinone A (1) exhibited potent inhibition of HCT-116 (human colon adenocarcinoma cell line) with an IC₅₀ value of 9.9×10^{-9} M [30].

In conclusion, *A. thermoflava* strain SMFA-103 isolated from the rhizosphere soil of sunflower (*Helianthus annuus* L.) was found to produce a promising bioactive extrolite, 1-methoxy-3-methyl-8-hydroxy-anthraquinone. This is the first report on this bioactive anthraquinone from *A. thermoflava* strain SFMA-103, which exhibited anti-tumor activity against a panel of cancer cell lines and showed non-toxic effect to normal human embryonic kidney cell line. It also scavenged DPPH free radicals, superoxide anions, nitric oxide radicals and lipid peroxy radicals. The antitumor and antioxidant activities exhibited by 1-methoxy-3-methyl-8-hydroxy-anthraquinone seems to be promising and may find plausible application in biotechnological and pharmaceutical fields.

Acknowledgments

The authors acknowledge the financial assistance provided to PM, YP and BS in the form of Senior Research Fellowships by Council of Scientific and Industrial Research (CSIR), New Delhi, India.

Conflict of Interest

We declare that there is no conflict of interest with any researcher or funding agency.

References

- Lancini G, Lorenzetti R. 1993. *Biotechnology of antibiotics and other bioactive microbial metabolites*. pp. 49-57. Plenum Press, New York and London.
- Lazzarini A, Cavaletti L, Toppo G, Marinelli F. 2000. Rare genera of actinomycetes as potential producers of new antibiotics. *Antonie van Leeuwenhoek* **78**: 399-405.
- Jensen PR, Mincer TJ, Williams PG, Fenical W. 2005. Marine actinomycete diversity and natural product discovery. *Antonie van Leeuwenhoek* **87**: 43-48.
- Caro Y, Anamale L, Fouillaud M, Laurent P, Petit T, Dufosse L. 2012. Natural hydroxyanthraquinoid pigments as potent food grade colorants: an overview. *Nat. Prod. Bioprospect.* **2**: 174-193.
- Byrstrykh LV, Fernández-Moreno MA, Herrema JK, Malpartida F, Hopwood DA, Dukhuizen L. 1996. Production of actinorhodin-related "blue-pigments" by *Streptomyces coelicolor* A3(2). *J. Bacteriol.* **178**: 2238-2244.
- Clark B, Capon RJ, Stewart M, Lacey E, Tennant S, Gill JH. 2004. Blanchequinone: A new anthraquinone from an Australian *Streptomyces* sp. *J. Nat. Prod.* **67**: 1729-1731.
- Adinarayana G, Venkateshan MR, Bapiraju VVSNK, Sujatha P, Premkumar J, Ellaiah P, Zeeck A. 2006. Cytotoxic compounds from the marine actinobacterium *Streptomyces corchorusii* AUBN(1)/7. *Russ. J. Bioorg. Chem.* **32**: 295-300.
- Igarashi Y, Trujillo M E, Martinez-Molina E, Yanase S, Miyana S, Obata T, *et al.* 2007. Antitumor anthraquinones from an endophytic actinomycete *Micromonospora lupini* sp. nov. *Bioorg. Med. Chem. Lett.* **17**: 3702-3705.
- Xue CM, Tian L, Lin WH, Deng ZW. 2009. Anthraquinone derivatives from *Micromonospora rhodorangea*. *Nat. Prod. Res.* **23**: 533-538.
- Balachandran C, Arun Y, Duraipandiyan V, Ignacimuthu S, Balakrishna K, Al-Dhabi NA. 2014. Antimicrobial and cytotoxicity properties of 2,3-dihydroxy-9,10-anthraquinone isolated from *Streptomyces galbus* (ERINLG-127). *Appl. Biochem. Biotechnol.* **172**: 3513-3528.
- Balachandran C, Duraipandiyan V, Arun Y, Sangeetha B, Emi N, Al-Dhabi NA, *et al.* 2016. Isolation and characterization of 2-hydroxy-9,10-anthraquinone from *Streptomyces olivochromogenes* (ERINLG-261) with antimicrobial and antiproliferative properties. *Revista Brasileira de Farmacognosia* **26**: 285-295.
- Shirling EB, Gottlieb D. 1996. Methods for characterization of *Streptomyces* species. *Int. J. Syst. Bacteriol.* **16**: 313-340.
- Chun J, Kim SB, Oh YK, Seong CN, Lee DH, Bae KS, *et al.* 1999. *Amycolatopsis thermoflava* sp. nov., a novel soil actinomycete from Hainan Island, China. *Int. J. Syst. Bacteriol.* **49**: 1369-1373.
- Haque SK, Sen SK, Pal SC. 1992. Screening and identification of antibiotic producing strains of *Streptomyces*. *Hindustan Antibiot. Bull.* **4**: 76-83.
- Rainey FA, Rainey NW, Kroppenstedt RM, Stackebrandt E. 1996. The genus *Nocardopsis* represents a phylogenetically coherent taxon and a distinct actinomycete lineage: proposal of *Nocardio-opsiaceae* fam. nov. *Int. J. Syst. Bacteriol.* **46**: 1088-1092.
- Tamura K, Nei M. 1983. Estimation of the number of nucleotide substitutions in the control region of mitochondrial DNA in humans and chimpanzees. *Mol. Biol. Evol.* **10**: 512-526.
- Tamura K, Stecher G, Peterson D, Filipiński A, Kumar S. 2013. MEGA6: Molecular Evolutionary Genetic Analysis version 6.0. *Mol. Biol. Evol.* **30**: 2725-2729.
- Moon JH, Terao J. 1998. Antioxidant activity of caffeic acid and dihydrocaffeic acid in lard and human low-density lipoprotein. *J. Agric. Food Chem.* **46**: 5062-5065.
- Bors W, Heller W, Michel C, Saran M. 1990. Flavonoids as antioxidants: determination of radical-scavenging efficiencies. *Methods Enzymol.* **186**: 343-355.
- Liu F, Ooi VE, Chang ST. 1997. Free radical scavenging activities of mushroom polysaccharide extracts. *Life Sci.* **60**: 763-771.
- Zhang EX, Yu LJ. 1997. Studies on polysaccharide from *Sargassum thunbergii* for its ability to scavenge active oxygen species. *Chin. J. Mar. Drugs* **3**: 1-4.
- Marcocci L, Packer L, Droy-Lefaix MT, Sekaki A, Gardes-Albert M. 1994. Antioxidant action of *Ginkgo biloba* extract EGB 761. *Methods Enzymol.* **234**: 462-475.
- Mosmann T. 1983. Rapid colorimetric assay for cellular growth and survival; application to proliferation and cytotoxicity assays. *J. Immunol. Methods* **65**: 55-63.
- Kim B, Sahin N, Tan GYA, Zakrzewska-Czerwinska J, Goodfellow M. 2002. *Amycolatopsis eurytherma* sp. nov., a thermophilic actinomycete isolated from soil. *Int. J. Syst. Evol. Microbiol.* **52**: 889-894.
- Huang Q, Lu G, Shen HM, Chung MC, Ong CN. 2007. Anti-cancer properties of anthraquinones from rhubarb. *Med. Res. Rev.* **27**: 609-630.
- Mao H, Schnetz-Boutaud NC, Weisenseel JP, Marnett LJ, Stone MP. 1999. Duplex DNA catalyzes the chemical rearrangement of a malondialdehyde deoxyguanosine adduct. *Proc. Nat. Acad. Sci. USA* **96**: 6615-6620.
- Marnett LJ. 1999. Lipid peroxidation - DNA damage by malondialdehyde. *Mutat. Res.* **424**: 83-95.
- Hu Y, Martinez ED, MacMillan JB. 2012. Anthraquinones from a marine-derived *Streptomyces spinoverrucosus*. *J. Nat. Prod.* **75**: 1759-1764.
- Raju R, Gromyko O, Fedorenko V, Herrmann J, Luzhetskyy A, Müller R. 2013. Rubimycinone A, a new anthraquinone from a terrestrial *Streptomyces* sp. *Tetrahedron Lett.* **54**: 900-902.
- Huang YF, Tian L, Fu HW, Hua HM, Pei YH. 2006. One new anthraquinone from marine *Streptomyces* sp. FX-58. *Nat. Prod. Res.* **20**: 1207-1210.
- Murphy BT, Narender T, Kauffman CA, Woolery M, Jensen PR, Fenical W. 2010. Saliniquinones A-F, new members of the highly cytotoxic anthraquinone- γ -pyrones from the marine actinomycete *Salinispora arenicola*. *Aust. J. Chem.* **63**: 929-934.